NATIONAL ADVISORY COMMITTEE FOR AERONAUTICS

TECHNICAL NOTE

No. 1480

DETERMINATION OF PLATE COMPRESSIVE STRENGTHS

By George J. Heimerl

Langley Memorial Aeronautical Laboratory
Langley Field, Va.

Washington
December 1947

NATIONAL ADVISORY COMMITTEE FOR AERONAUTICS

TECHNICAL NOTE NO. 1480

DETERMINATION OF PLATE COMPRESSIVE STRENGTHS

By George J. Heimerl

SUMMARY

Results of local-instability tests of H-, Z-, and C-section plate assemblies of four extruded aluminum alloys and two magnesium alloys, obtained in an extensive investigation to determine plate compressive strengths of aircraft structural materials, are summarized. On the basis of the general relationships found between the plate compressive strengths and the compressive stress-strain curves, methods applicable to flat plates and based upon the use of the compressive stress-strain curve are suggested for determining the critical compressive stress and the average stress at maximum load.

INTRODUCTION

In the NACA investigation to determine the plate compressive strengths of a number of aircraft structural materials (references 1 to 7), local-instability tests were made of flat plate assemblies consisting of extruded sections and sections obtained by forming flat sheet. A correlation between plate buckling and compressive stress-strain curves was observed, and an experimental relationship was found to exist between the critical compressive stress and the average stress at maximum load. The results obtained for the sheet materials differed noticeably from those for the extruded materials apparently because of forming and curvature effects.

The purpose of the present paper is to summarize the essential results obtained for the plate compressive strengths of the extruded materials and to show methods by which flat plate compressive strengths may be determined in general from the compressive stress-strain curve for the material.

METHODS OF TESTING AND ANALYSIS

The methods of testing and analysis employed in the investigation (references 3 to 7) are briefly reviewed herein.

Testing.- The plate compressive strengths were determined from tests of flat plate assemblies consisting of H-, Z-, or C-sections so proportioned that the plate elements failed by local instability. (See fig. 1.) The plate assemblies were made from special H-section extrusions, and the cross-sectional proportions were varied by cutting off parts of the flanges. The lengths of the sections were chosen in such a way that the test results were essentially independent of length; that is, sufficiently long so that the increase in strength due to very short lengths was avoided and at the same time not so long as to incur the possibility of an Euler type of column failure. The lengths were also selected so as to obtain a convenient three-half-wave-buckling pattern which gave a pronounced cross-sectional distortion at the mid-length position (see reference 8 and fig. 1), except that in the high stress region reduced lengths were necessary in order to avoid Euler column failures. The experimental critical stress was taken as the stress corresponding to the critical load at the top of the knee of the load distortion curve as illustrated in figure 2. (For a discussion of initial curvature effects and the use of the "top-of-the-knee method," see reference 9.) The distortion was measured by various methods, and in the later tests, was recorded autographically together with the load. The average stress at maximum load was obtained from the maximum load recorded by the testing machine. The compressive stress-strain curves were obtained from tests of single-thickness specimens cut from the flanges and web at the ends of the H-section extrusions; the tests were made in a modified form of Montgomery-Templin type of compression fixture. (For technique in using this type of fixture, see reference 10.)

Analysis of compressive properties of material.- Because the tests of the compression specimens cut from the web and flanges of the extrusions showed that the properties varied both over the cross sections (see fig. 3) and along the lengths of the extrusions, the exact determination of a compressive stress-strain curve for correlation with the plate compressive strengths of the sections is difficult. The method used herein for obtaining a representative value of the compressive yield stress σ_{cy} for a cross section is based on the assumption that the test results for σ_{cy} for the flange and web material apply to the entire width of those respective elements and that a representative value for a cross section can be had by calculating a weighted average from the values of σ_{cy} for the flange and the web, taking into account the area of these elements. The compressive stress-strain curves shown herein were selected from the tests to show the upper and lower limits of the calculated over-all cross-sectional properties for the sections which had buckling stresses above the elastic range.

Analysis of buckling data.- In the presentation of the test data of references 1 to 7, the experimental critical compressive stress was plotted against the calculated elastic critical compressive stress σ_{cr}/η, as given by the equation

$$\frac{\sigma_{cr}}{\eta} = \frac{k_w \pi^2 E t_w^2}{12(1 - \mu^2) b_w^2} \qquad (1)$$

In equation (1), k_w is a nondimensional coefficient dependent upon plate proportions and edge conditions to be used with t_w and b_w, the thickness and width, respectively, of the web of the H-, Z-, and C-sections (see fig. 4 for method of dimensioning these extruded sections), μ is Poisson's ratio, E is Young's modulus, and η is a coefficient which is a measure of the reduced plate modulus ηE. (For stresses in the elastic range, $\eta = 1$, whereas above the elastic range, $\eta < 1$.) The purpose of this method of analysis was to afford a convenient way of determining empirically the variation of η with stress for use in evaluating plate-buckling strengths above the elastic range.

In the present paper, the method of presentation has been modified slightly from that in references 1 to 7 in that the experimental critical compressive stress has been plotted against the calculated elastic critical compressive strain ϵ_{cr} which is derived from equation (1) by dividing both sides by E and setting $\eta = 1$. Thus

$$\epsilon_{cr} = \frac{k_w \pi^2 t_w^2}{12(1 - \mu^2) b_w^2} \qquad (2)$$

By this method of analysis, it is possible to correlate plate buckling stress-strain curves directly with compressive stress-strain curves. Values of the nondimensional coefficients used in plate equations of the form given by equations (1) and (2) are found in the literature for individual plates with different edge conditions and are available in reference 11 in the form of charts for plate assemblies such as H-, Z-, C-, and rectangular-tube sections. It should be emphasized that the test results are for plates having length-width ratios sufficiently large so that the experimental values of σ_{cr} are essentially independent of length; values of k_w in reference 11 apply to this class of plates.

RESULTS AND CONCLUSIONS

The experimental results for the critical compressive stress σ_{cr} and the average stress at maximum load $\bar{\sigma}_{max}$ for the H-, Z-, and C-section plate assemblies (references 3 to 7) are given in figures 5 to 8 together with unpublished data on extruded ZK60A magnesium alloy. (Because the data were too numerous to reproduce clearly, many of the test points have been omitted.) The correlation with the compressive stress-strain curves for the material is shown in figures 5 and 6 by plotting the test results against the calculated elastic critical compressive strain ϵ_{cr}. The relationship between σ_{cr}, $\bar{\sigma}_{max}$, and the compressive yield stress σ_{cy} is shown in nondimensional form in figures 7 and 8.

For the H-sections (fig. 5), the test results for σ_{cr} above the elastic range tend to fall fairly close to the lower limit stress-strain curves with the exceptions of 75S-T, 14S-T, and 24S-T aluminum alloys. For 75S-T, the results are only a little below the lower limit curve, but for 14S-T, appreciably lower. The test results for 14S-T differed markedly from those for the other materials in that separate curves for H-sections and for Z- and C-sections were not obtained. The reason for this difference is not known, but may be due to the nonuniformity of the material. (See discussion, reference 6.) For 24S-T, however, the results for the H-sections appear to be close to an average of the upper and lower limit curves.

For the Z- and C-sections (fig. 6), the results for σ_{cr} above the elastic range generally tend to be somewhat lower than those for the corresponding H-sections (fig. 5) and fall slightly below the lower limit stress-strain curves with the exception of 24S-T for which the results are close to or slightly above the lower limit curve. This result may be due, to some extent, to the inadequacy of the method used for calculating the compressive properties applicable to the entire cross section upon which the selection of stress-strain curves in figures 5 and 6 was based. (See section entitled "Analysis of compressive properties of the material.")

In figures 7 and 8, the results of all the tests for the H-sections and for the Z- and C-sections, respectively, are given in nondimensional form by single curves relating σ_{cr} and $\bar{\sigma}_{max}$ in terms of σ_{cy}. For a given critical compressive stress, the curve for the Z- and C-sections (fig. 8) differs slightly from that for the H-sections (fig. 7) and indicates that $\bar{\sigma}_{max}$ is slightly greater for an H-section than for a Z- or C-section. This difference in $\bar{\sigma}_{max}$ for H-sections

and for Z- and C-sections corresponds somewhat to the difference found in σ_{cr} for these same sections and also probably stems in part from the inadequacy of the method used for determining the value of σ_{cy} that applies to the entire cross section. (See preceding paragraph with regard to σ_{cr}.) A significant result indicated in figures 7 and 8 is that, for stresses above about $\frac{3}{4}\sigma_{cy}$, $\bar{\sigma}_{max}$ is only a little greater than σ_{cr}, but for stresses below $\frac{3}{4}\sigma_{cy}$, $\bar{\sigma}_{max}$ and σ_{cr} differ appreciably. This result is also borne out in figures 5 and 6 where, for the different materials, values of $\bar{\sigma}_{max}$ run only a little above those for σ_{cr} in the high-stress region but differ appreciably in the low-stress region.

From figures 5 to 8, the following conclusions may be drawn with regard to the critical compressive stress and the average stress at maximum load for extruded H-, Z-, and C-section plate assemblies:

(1) Because of the general agreement between the compressive stress-strain curves and the test results for σ_{cr} when plotted against calculated values of ϵ_{cr}, the reduced modulus of elasticity for plate buckling may be approximated by the secant modulus. (The use of the secant modulus has previously been suggested in reference 12.) Consequently, the critical compressive stress may be determined for practical purposes either directly from the compressive stress-strain curve for the material, given the calculated value of ϵ_{cr}, or by the secant-modulus method in which E_{sec} is substituted for the reduced modulus ηE in the plate-buckling equation

$$\sigma_{cr} = \frac{k_w \pi^2 E_{sec} t_w^2}{12(1 - \mu^2) b_w^2} \tag{3}$$

The results obtained by the foregoing methods tend to be somewhat unconservative in most cases unless a lower limit compressive stress-strain curve is used for the determination. The results obtained for Z- and C-sections will probably be less accurate and somewhat more unconservative than those for H-sections.

(2) For stresses greater than $\frac{3}{4}\sigma_{cy}$, values of $\bar{\sigma}_{max}$ are only slightly greater than σ_{cr} (see figs. 7 and 8) and generally

superimpose more closely on an average of the upper and lower limit stress-strain curves for the material than do values of σ_{cr}. (See figs. 5 and 6.) For this reason, the secant-modulus method can also be applied to the approximate determination of $\bar{\sigma}_{max}$ in this high stress region with results which tend to be somewhat more accurate and conservative than for the similar determination of σ_{cr}, particularly if a lower limit stress-strain curve is used.

Thus for $\bar{\sigma}_{max} \geq \frac{3}{4}\sigma_{cy}$,

$$\bar{\sigma}_{max} = \frac{k_w \pi^2 E_{sec} t_w^2}{12(1 - \mu^2) b_w^2} \tag{4}$$

(3) For stresses less than $\frac{3}{4}\sigma_{cy}$, the relationships shown in figures 7 and 8 between $\bar{\sigma}_{max}$, σ_{cr}, and σ_{cy} may be used to determine $\bar{\sigma}_{max}$. These relationships, which are nearly the same for the Z- and C-sections as for the H-sections, are for $\bar{\sigma}_{max} \leq \frac{3}{4}\sigma_{cy}$:

For H-sections,

$$\frac{\sigma_{cr}}{\sigma_{cy}} = 0.75 \left(\frac{\sigma_{cr}}{\bar{\sigma}_{max}} \right)^{5/4} \tag{5}$$

For Z- and C-sections,

$$\frac{\sigma_{cr}}{\sigma_{cy}} = 0.72 \left(\frac{\sigma_{cr}}{\bar{\sigma}_{max}} \right)^{5/4} \tag{6}$$

Solving equations (5) and (6) for $\bar{\sigma}_{max}$ gives for $\bar{\sigma}_{max} \leq \frac{3}{4}\sigma_{cy}$:

For H-sections,

$$\bar{\sigma}_{max} = 0.80 \left(\sigma_{cr} \sigma_{cy}^4 \right)^{1/5} \tag{7}$$

For Z- and C-sections,

$$\bar{\sigma}_{max} = 0.77 \left(\sigma_{cr} \sigma_{cy}^4 \right)^{1/5} \tag{8}$$

The foregoing conclusions apply specifically to H-, Z-, and C-section plate assemblies. The results, however, may be generalized somewhat as follows: In view of the general relationship found between the critical compressive stress for the H-, Z-, and C-section plate assemblies and the compressive stress-strain curve for the different materials, it seems reasonable to expect about the same relationship for other types of plate assemblies such as skin-stiffener combinations. Evidence that this supposition is warranted is afforded by some unpublished data on Z-stiffened compression panels. In general, the indications are that the reduced modulus is probably a little lower than the secant modulus obtained from an average stress-strain curve for the material. With regard to $\overline{\sigma}_{max}$, available information on Z-stiffened panels indicates a correlation with the stress-strain curve similar to that found for H-, Z-, and C-sections for stresses above $\frac{3}{4}\sigma_{cy}$. For stresses below $\frac{3}{4}\sigma_{cy}$, however, relations obtained for σ_{max} for H-, Z-, and C-sections apparently cannot be expected to apply to radically different types of plate assemblies.

Langley Memorial Aeronautical Laboratory
National Advisory Committee for Aeronautics
Langley Field, Va., July 22, 1947

REFERENCES

1. Lundquist, Eugene E., Schuette, Evan H., Heimerl, George J., and Roy, J. Albert: Column and Plate Compressive Strengths of Aircraft Structural Materials. 24S-T Aluminum-Alloy Sheet. NACA ARR No. L5F01, 1945.

2. Heimerl, George J., and Roy, J. Albert: Column and Plate Compressive Strengths of Aircraft Structural Materials. 17S-T Aluminum-Alloy Sheet. NACA ARR No. L5F08, 1945.

3. Heimerl, George J., and Roy, J. Albert: Column and Plate Compressive Strengths of Aircraft Structural Materials. Extruded 75S-T Aluminum Alloy. NACA ARR No. L5F08a, 1945.

4. Heimerl, George J., and Roy, J. Albert: Column and Plate Compressive Strengths of Aircraft Structural Materials. Extruded 24S-T Aluminum Alloy. NACA ARR No. L5F08b, 1945.

5. Heimerl, George J., and Fay, Douglas P.: Column and Plate Compressive Strengths of Aircraft Structural Materials. Extruded R303-T Aluminum Alloy. NACA ARR No. L5H04, 1945.

6. Heimerl, George J., and Niles, Donald E.: Column and Plate Compressive Strengths of Aircraft Structural Materials. Extruded 14S-T Aluminum Alloy. NACA ARR No. L6C19, 1946.

7. Heimerl, George J., and Niles, Donald E.: Column and Plate Compressive Strengths of Aircraft Structural Materials. Extruded O-1HTA Magnesium Alloy. NACA TN No. 1156, 1947.

8. Heimerl, George J., and Roy, J. Albert: Determination of Desirable Lengths of Z- and Channel-Section Columns for Local-Instability Tests. NACA RB No. L4H10, 1944.

9. Hu, Pai C., Lundquist, Eugene E., and Batdorf, S. B.: Effect of Small Deviations from Flatness on Effective Width and Buckling of Plates in Compression. NACA TN No. 1124, 1946.

10. Kotanchik, Joseph N., Woods, Walter, and Weinberger, Robert A.: Investigation of Methods of Supporting Single-Thickness Specimens in a Fixture for Determination of Compressive Stress-Strain Curves. NACA RB No. L5E15, 1945.

11. Kroll, W. D., Fisher, Gordon P., and Heimerl, George J.: Charts for Calculation of the Critical Stress for Local Instability of Columns with I-, Z-, Channel, and Rectangular-Tube Section. NACA ARR No. 3K04, 1943.

12. Gerard, George: Secant Modulus Method for Determining Plate Instability above the Proportional Limit. Jour. Aero. Sci., vol. 13, no. 1, Jan. 1946, pp. 38-44 and 48.

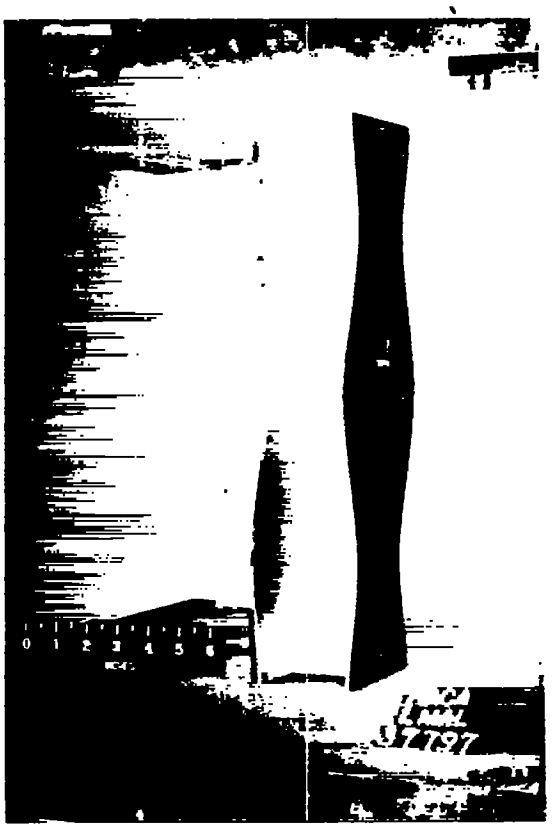

Figure 1.- Local instability for an H-section under test.

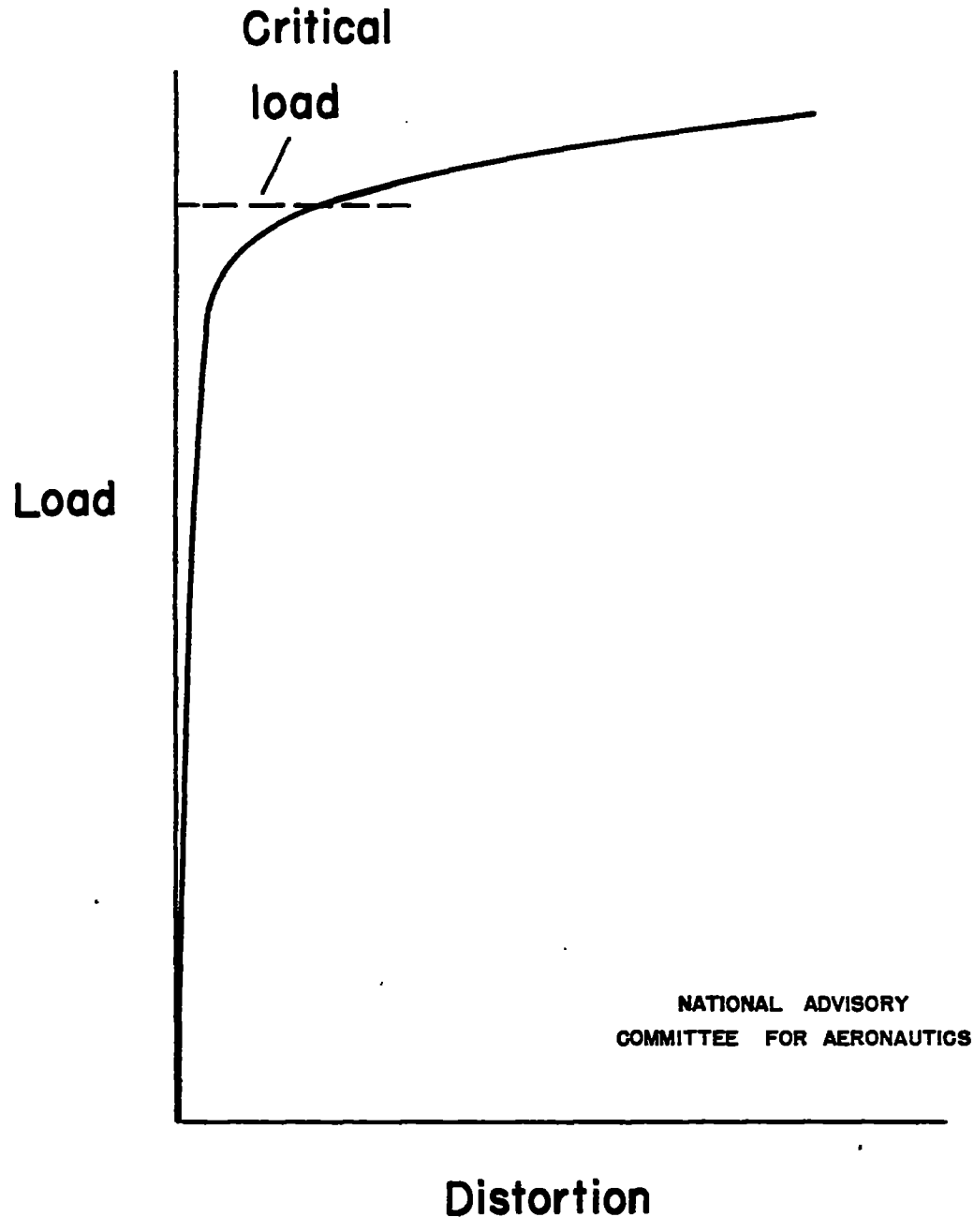

Figure 2.— Illustrative load-distortion curve.

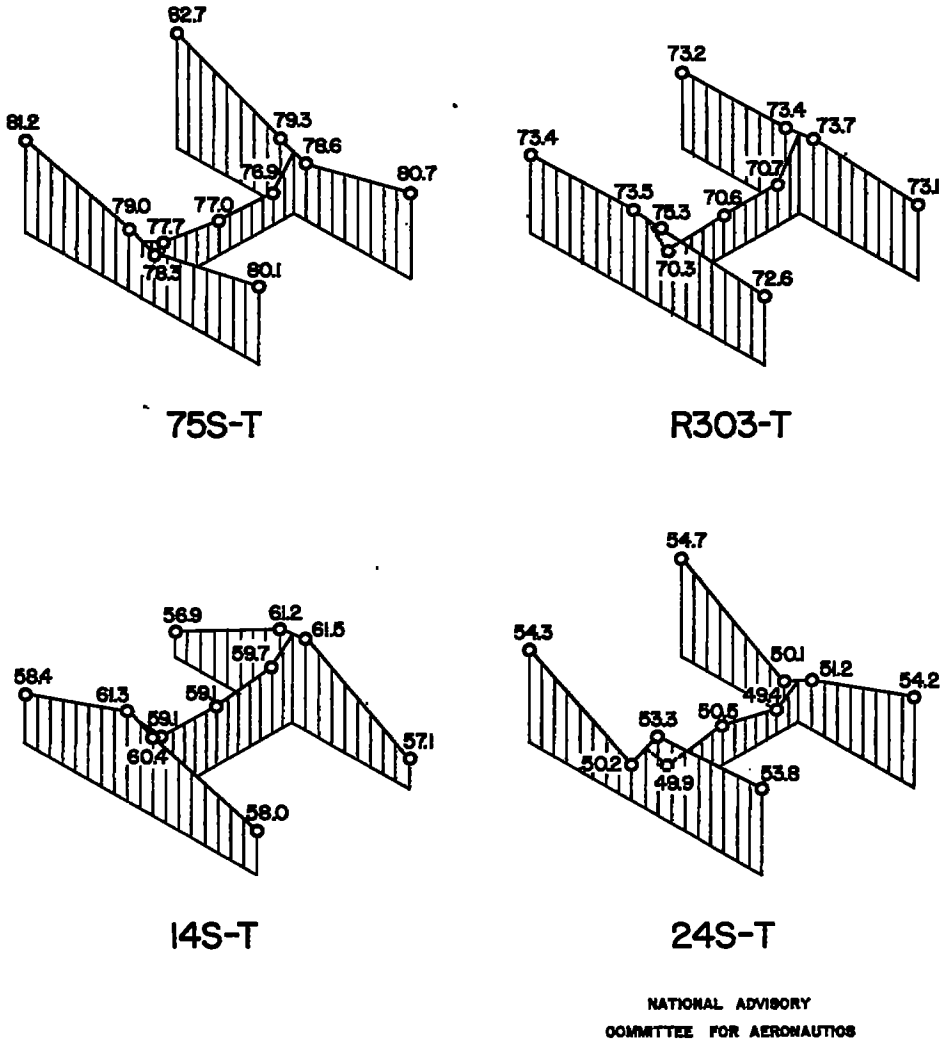

Figure 3.- Variction of the compressive yield stress in ksi over a single H-cross section for four extruded aluminum alloys.

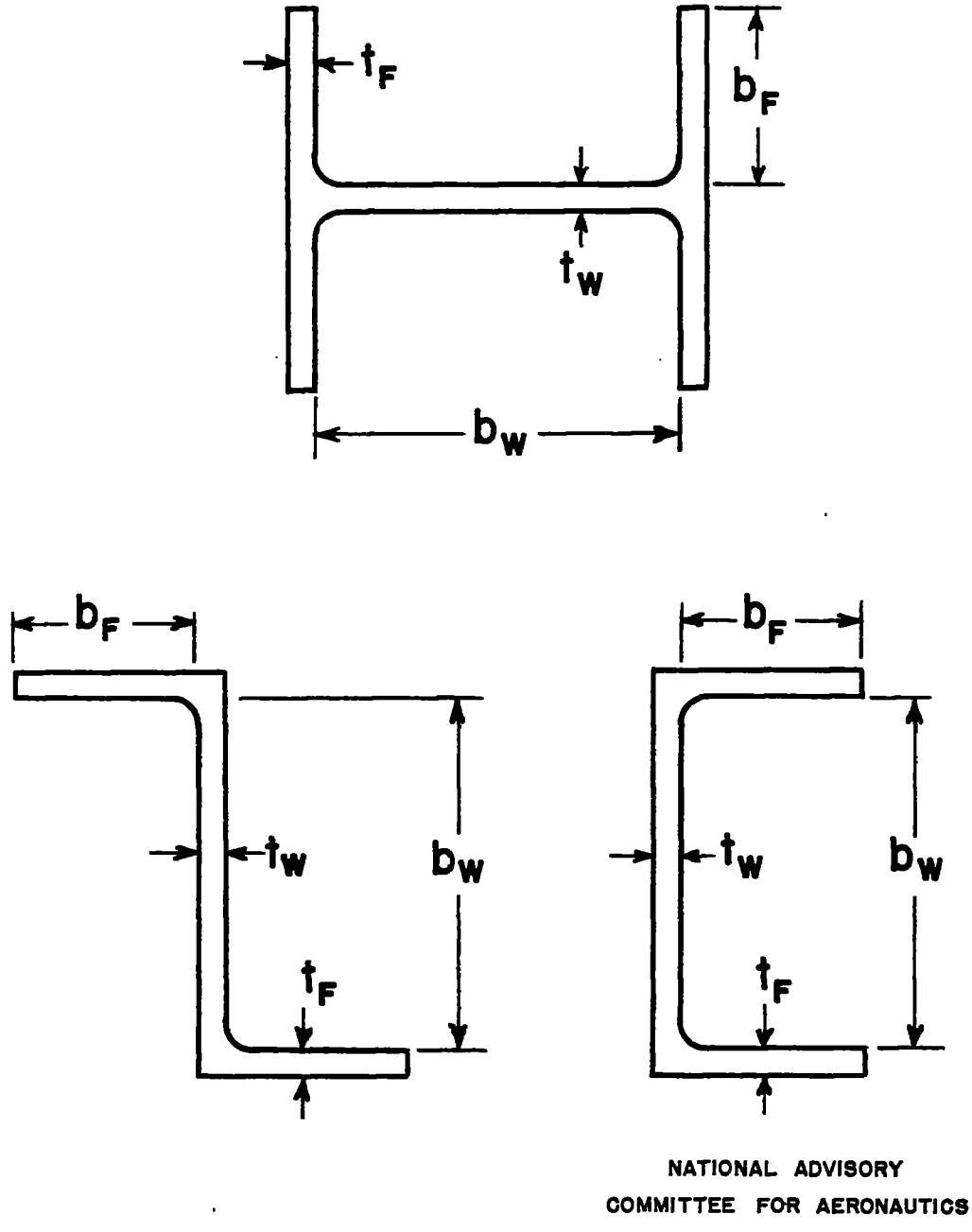

Figure 4. — Method of dimensioning extruded H-, Z-, and C-sections.

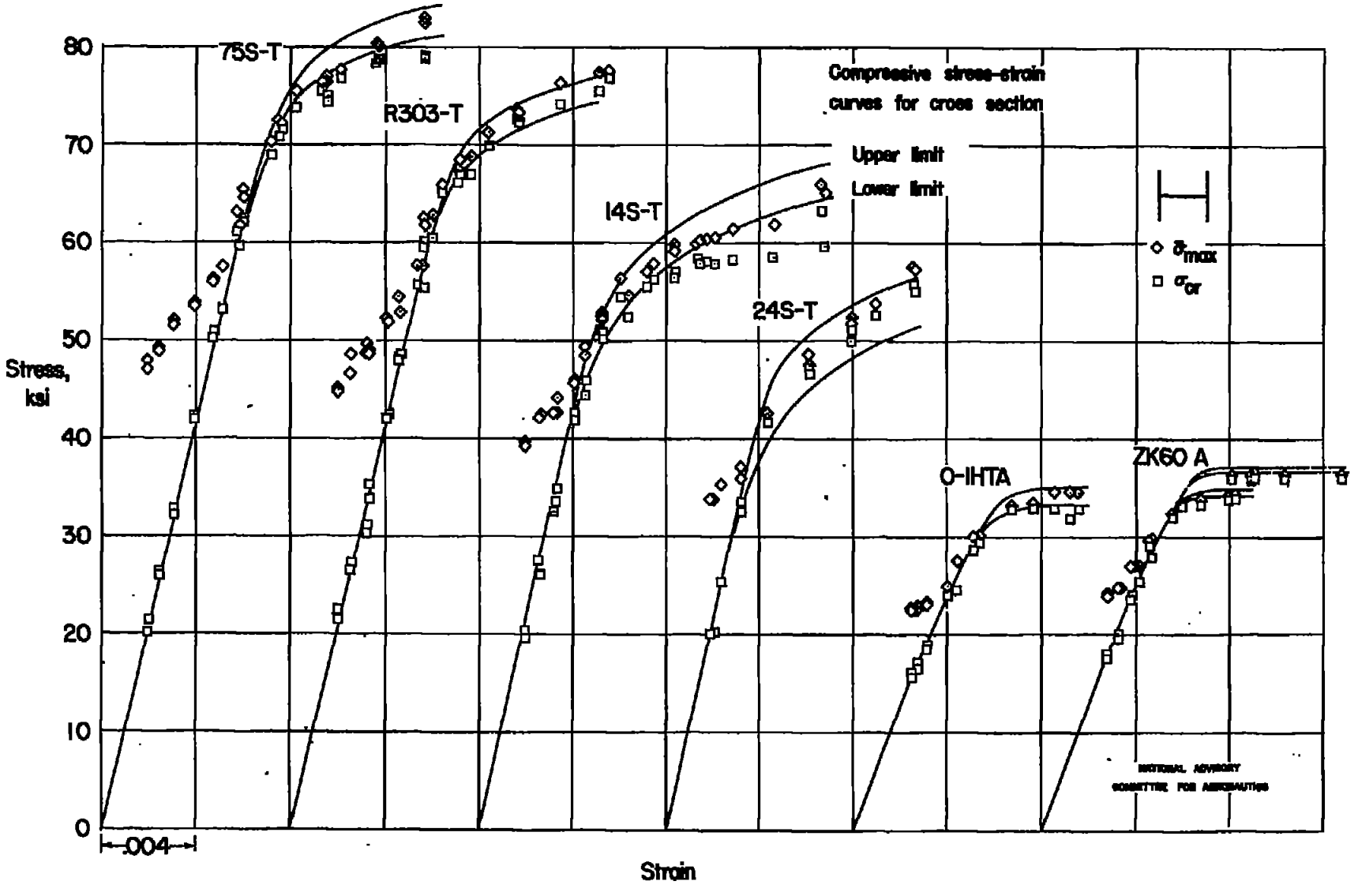

Figure 5. - Correlation of plate compressive test results with compressive stress-strain curves for extruded H-sections of various aluminum and magnesium alloys. (Calculated elastic critical compressive strain used for the plate tests.)

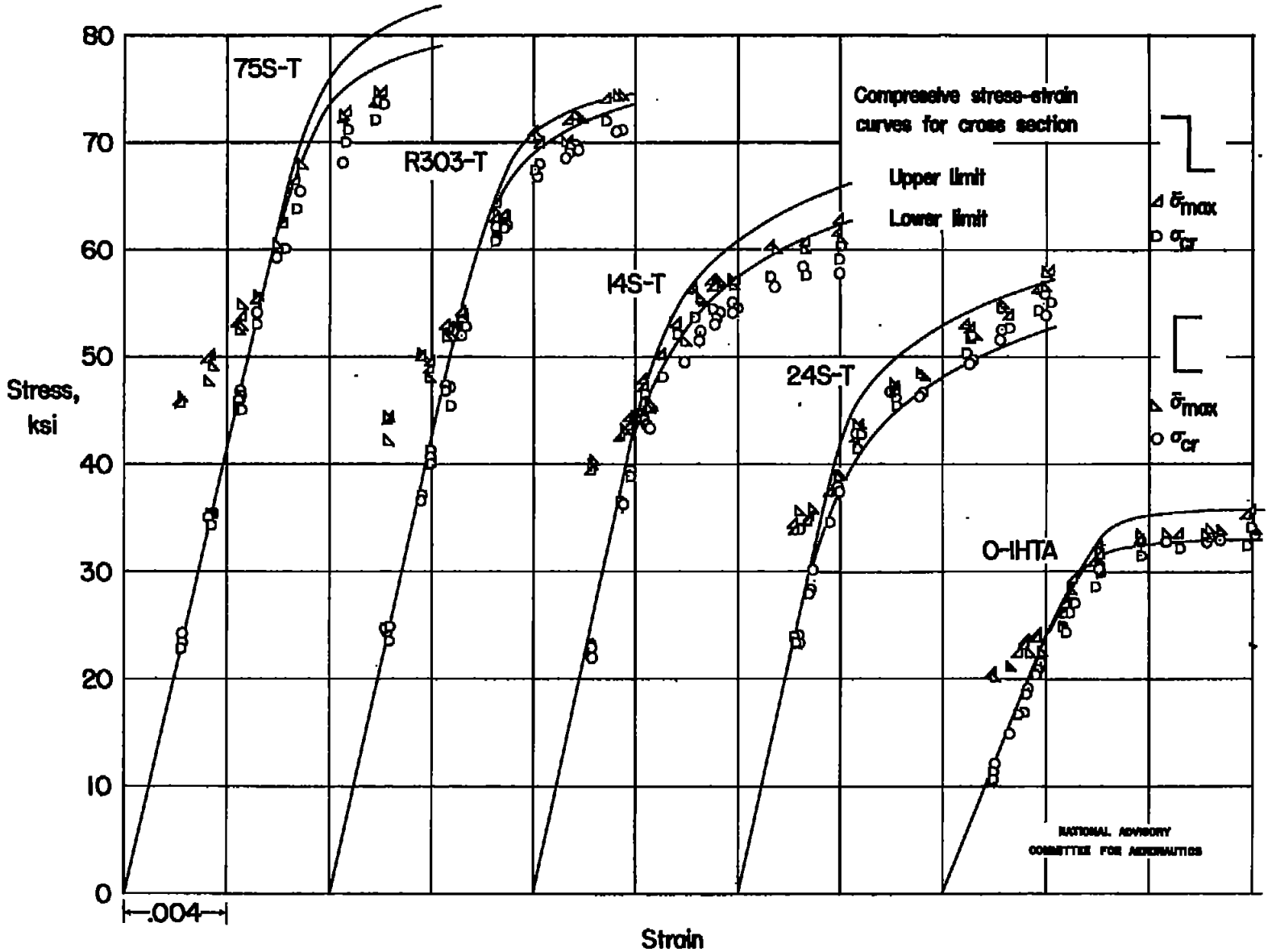

Figure 6.- Correlation of plate compressive test results for extruded Z- and C-sections of various aluminum and magnesium alloys. (Calculated elastic critical compressive strain used for plate tests)

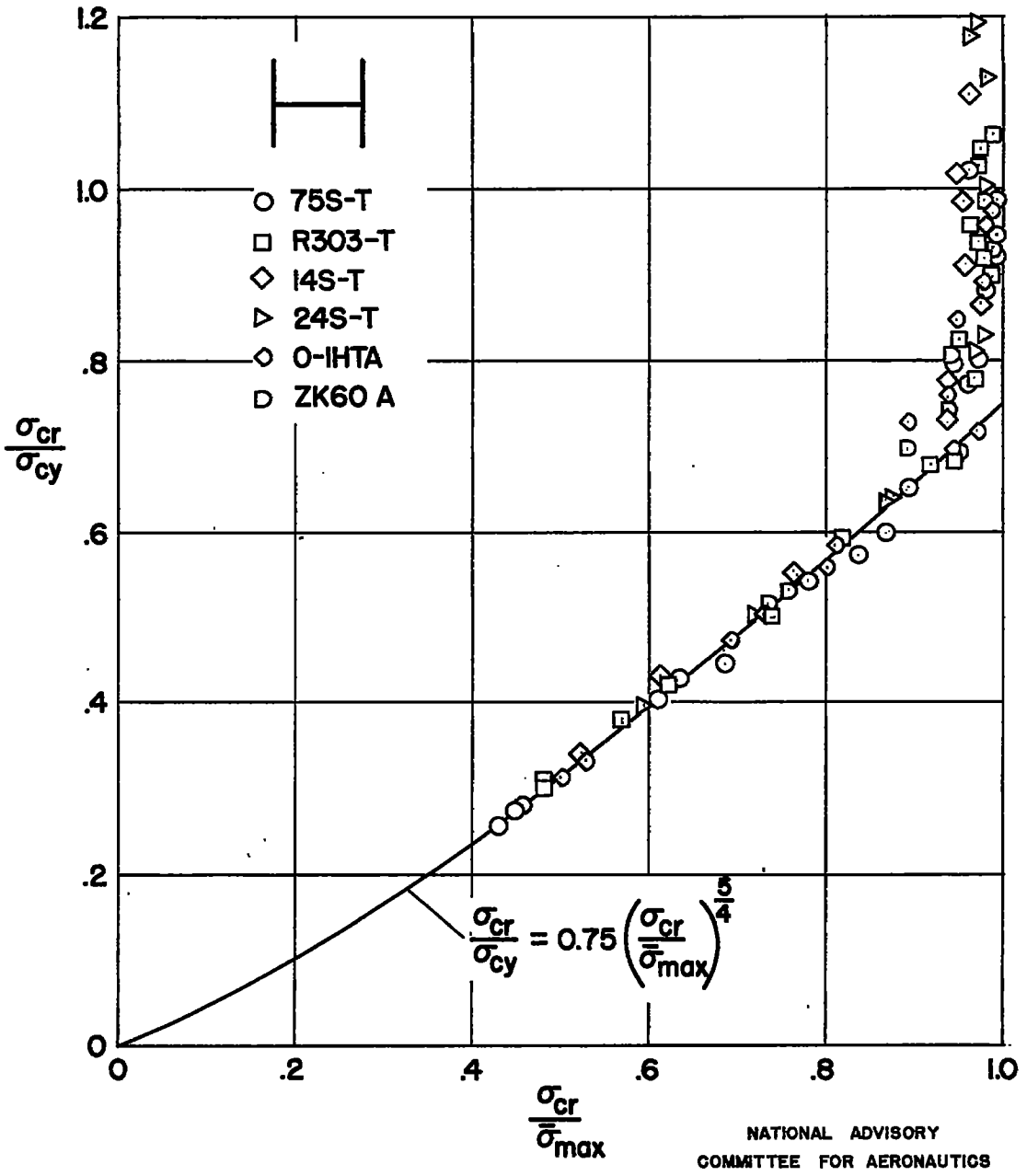

Figure 7. — Experimental relationship between the critical compressive stress σ_{cr}, the average stress at maximum load $\bar{\sigma}_{max}$, and the compressive yield stress σ_{cy} for extruded H-section plate assemblies of various aluminum and magnesium alloys.

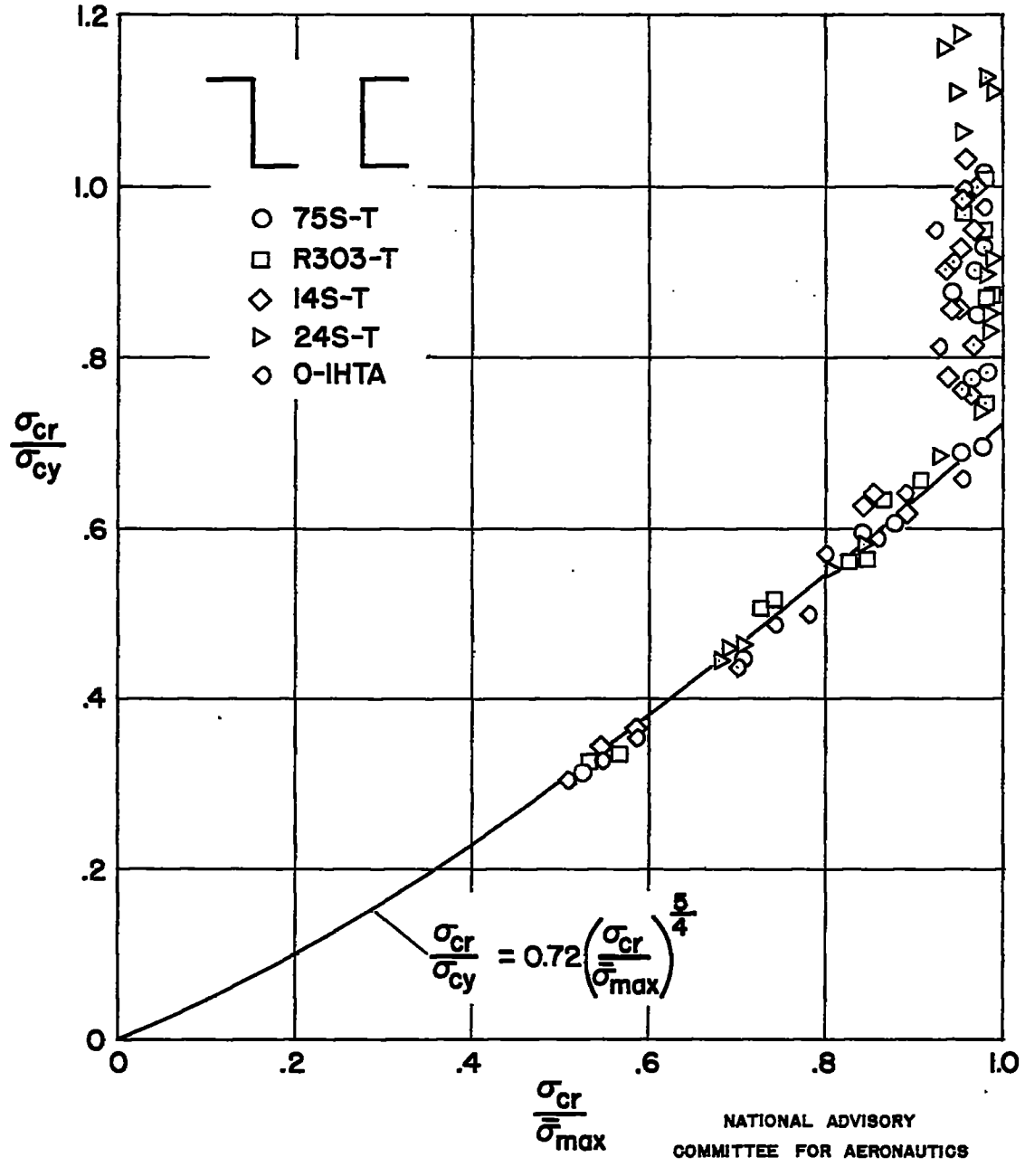

Figure 8.— Experimental relationship between the critical compressive stress σ_{cr}, the average stress at maximum load $\bar{\sigma}_{max}$, and the compressive yield stress σ_{cy} for extruded Z- and C-section plate assemblies of various aluminum and magnesium alloys.